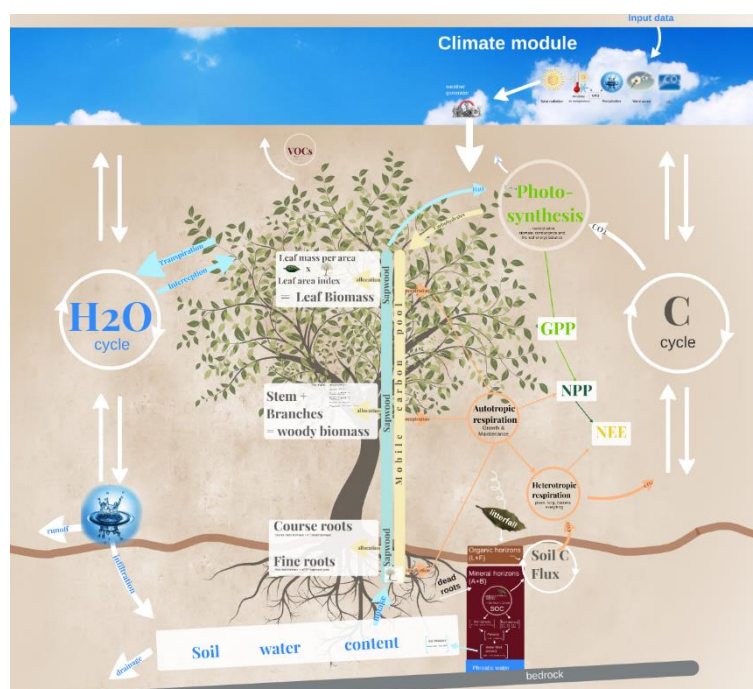


Supplementary Material

Gains or Losses in Forest Productivity under Climate Change? The Uncertainty of CO₂ Fertilization and Climate Effects

Supplementary Figures

a)



b)

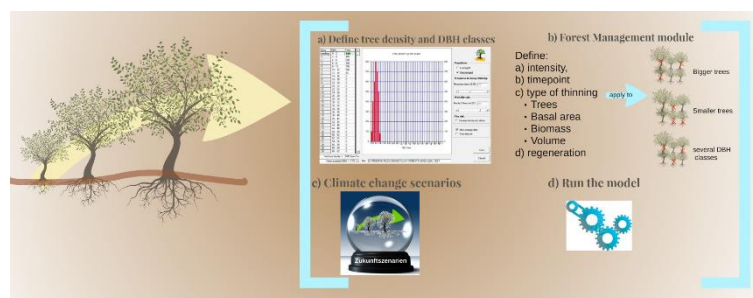


Figure S1. Schematic overview of GOTILWA+ of the ecophysiological and bio-geochemical growth module (a) and the forest management module (b). More details on each module can be found online by zooming in each module of the dynamic scheme available at <https://prezi.com/to-nd8yjmbaa/gotilwa-a-process-based-forest-growth-model>.

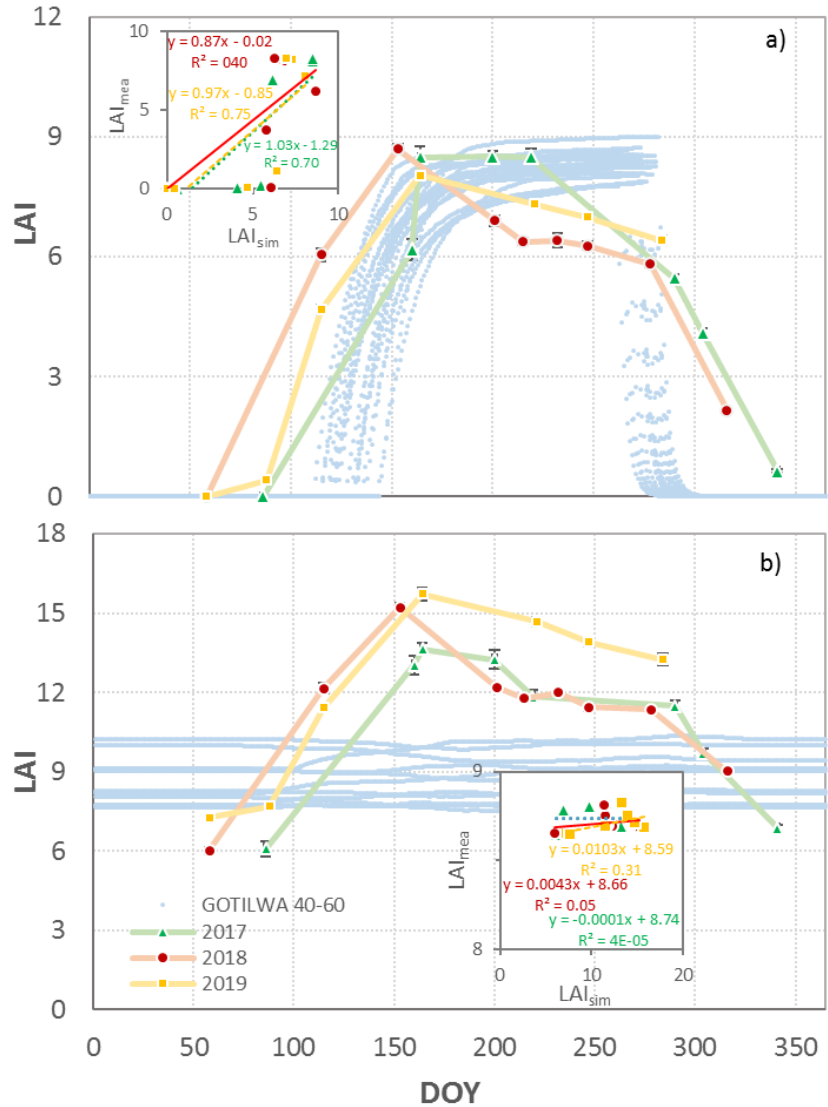


Figure S1. Measured leaf area index (LAI in m² m⁻²) of beech (a) and fir (b) at Freiamt at the day of the year (DOY) 2017, 2018 and 2019 and simulated LAI in GOTILWA+ at stand age 40 to 60 years (GOTILWA 40-60) (age range of the experimental forest) for (a) beech and (b) fir. In-built scatter plots show the regression equation and R² of measured (LAI_{mea}) versus simulated LAI (LAI_{sim}). LAI_{sim} is calculated as the mean from the 20 years for stand age 40 to 60 at the same DOY as for LAI_{mea}.

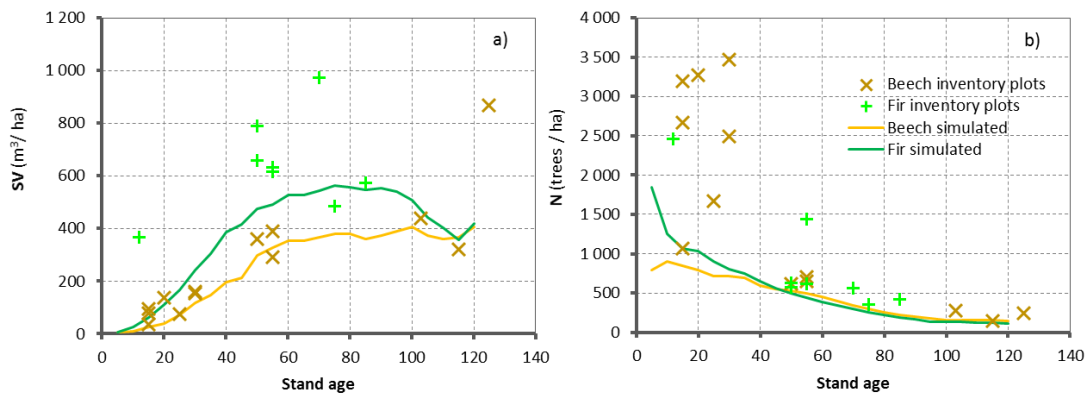


Figure S3. Standing wood volume (a) (SV, overbark in m³ ha⁻¹) and tree density (b) (N) of modelled stands and of inventory plots nearby the Freiamt experimental site.

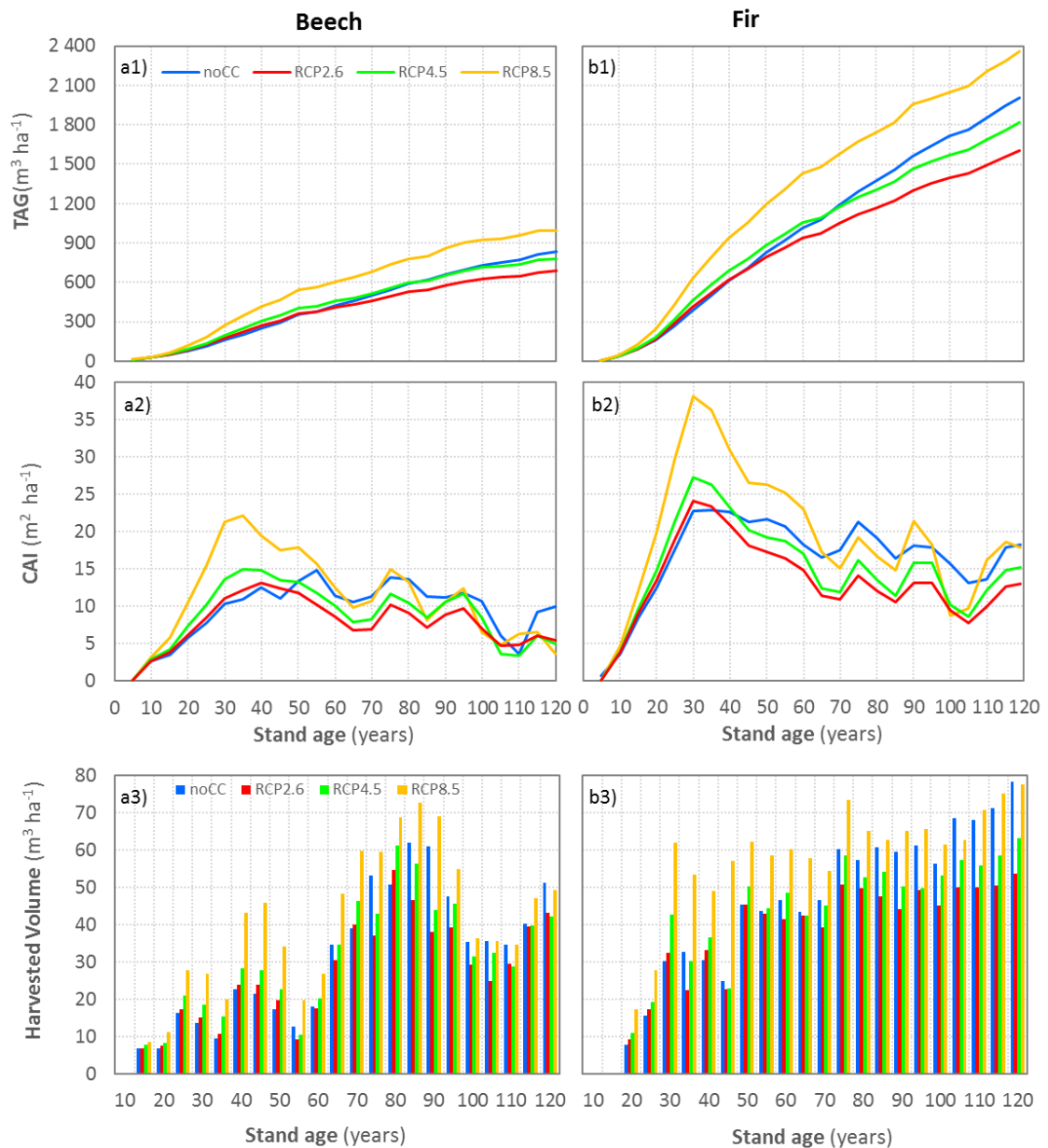


Figure S4. Effect of four climate scenarios (noCC, RCP2.6, RCP4.5, RCP8.5) on total accumulated growth (TAG) (1) and current annual increment (CAI) (2) and harvesting volume (HV) of beech (**a**) and fir (**b**). For the noCC scenario, a climate file of 120 was generated with an in-built weather generator in GOTILWA+ using climate data of the past 40 years from a nearby meteorological weather station with constant CO₂ concentration (370 ppm - global mean of 2018). For the three climate change scenarios RCP2.6, RCP4.5 and RCP8.5, changes in temperature, precipitation and CO₂ were applied to the generated climate file - according to the MPI-ESM-LR global circulation model.

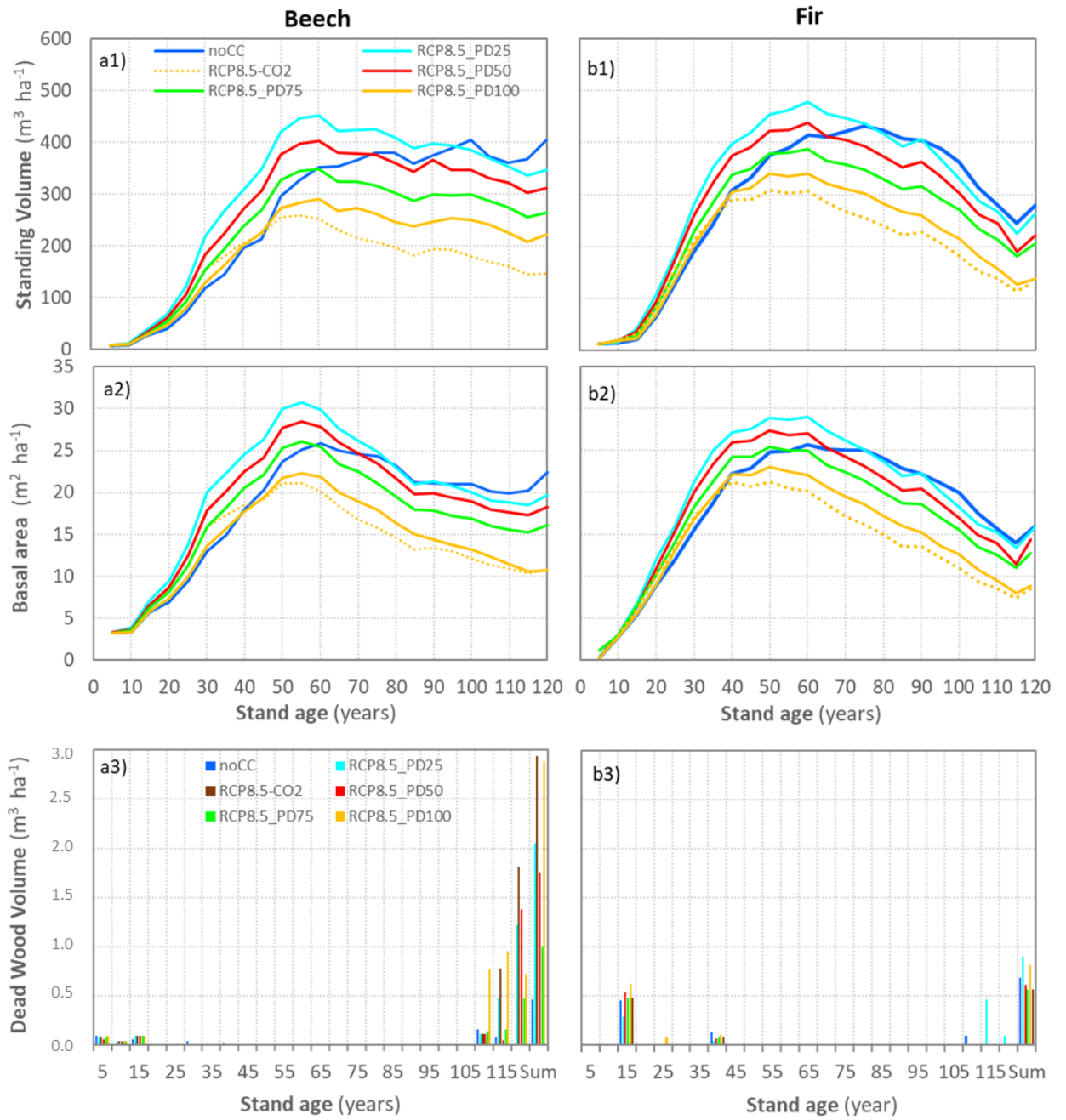


Figure S5. Effect of the climate change scenario RCP8.5 with constant CO₂ concentration (370 ppm - global mean of 2018) (RCP8.5-CO₂) and with increasing CO₂ concentration assuming photosynthetic downregulation by 25, 50, 75 and 100% (RCP8.5_PD25, RCP8.5_PD50, RCP8.5_PD75, RCP8.5_PD100) on standing volume (1), basal area (2), and dead wood volume (3) of beech (a) and fir (b). The climate scenario noCC is displayed for comparison assuming no change in precipitation and temperature and constant CO₂ concentration. The climate data was generated with an in-built weather generator in GOTILWA+ with climate data of the past 43 years from a nearby meteorological weather station. The simulations started with juvenile forests (stand age 0), which corresponds to simulation year 2000.

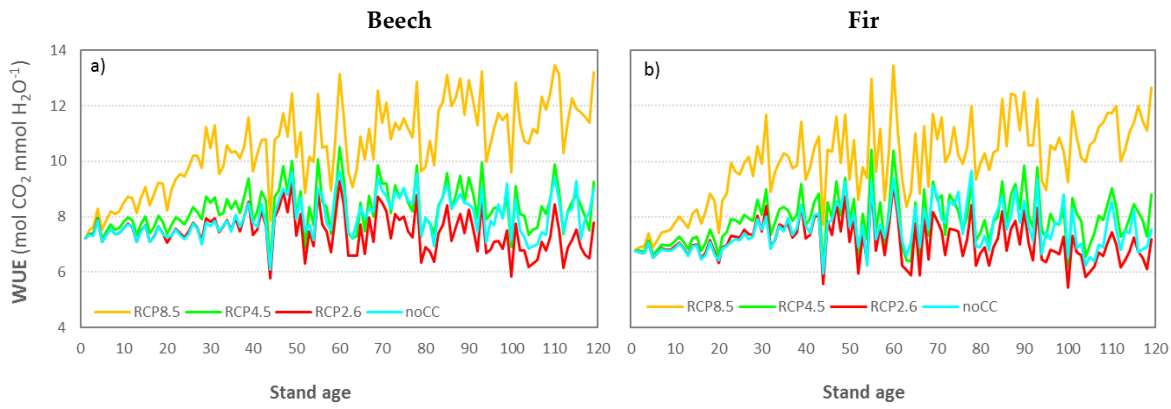


Figure S6. Effect of four climate scenarios (noCC, RCP2.6, RCP4.5, RCP8.5) on water-use efficiency of beech (a) and fir (b)). For the noCC scenario, a climate file of 120 was generated with an in-built weather generator in GOTILWA+ using climate data of the past 40 years from a nearby meteorological weather station with constant CO₂ concentration (370 ppm - global mean of 2018). For the three climate change scenarios RCP2.6, RCP4.5 and RCP8.5, changes in temperature, precipitation and CO₂ were applied to the generated climate file according to the MPI-ESM-LR global circulation model. The simulations started with juvenile forests (stand age 0), which corresponds to simulation year 2000.

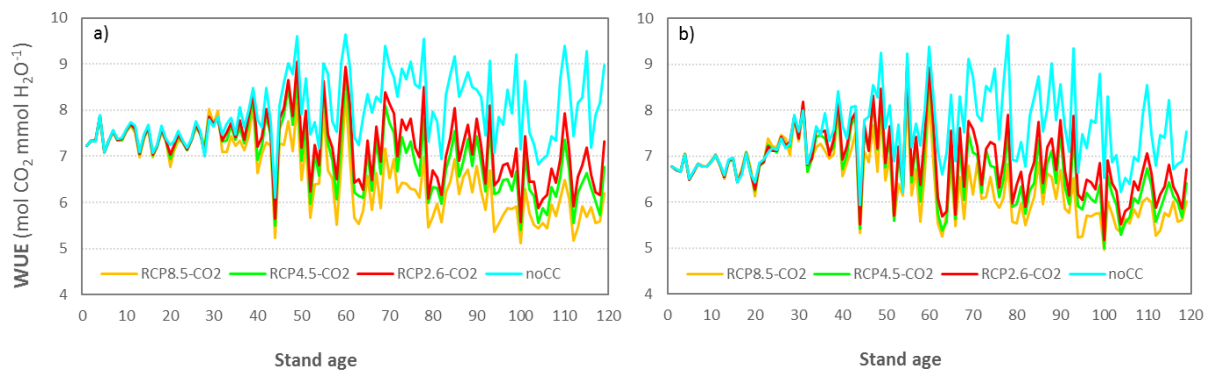


Figure S7. Effect of four climate scenarios (noCC, RCP2.6, RCP4.5, RCP8.5) with constant CO₂ concentration (370 ppm - global mean of 2018) on water-use efficiency of beech (a) and fir (b)). For the noCC scenario, a climate file of 120 was generated with an in-built weather generator in GOTILWA+ using climate data of the past 40 years from a nearby meteorological weather station. For the three climate change scenarios RCP2.6, RCP4.5 and RCP8.5, changes in temperature, precipitation and CO₂ were applied to the generated climate file according to the MPI-ESM-LR global circulation model. The simulations started with juvenile forests (stand age 0), which corresponds to simulation year 2000.

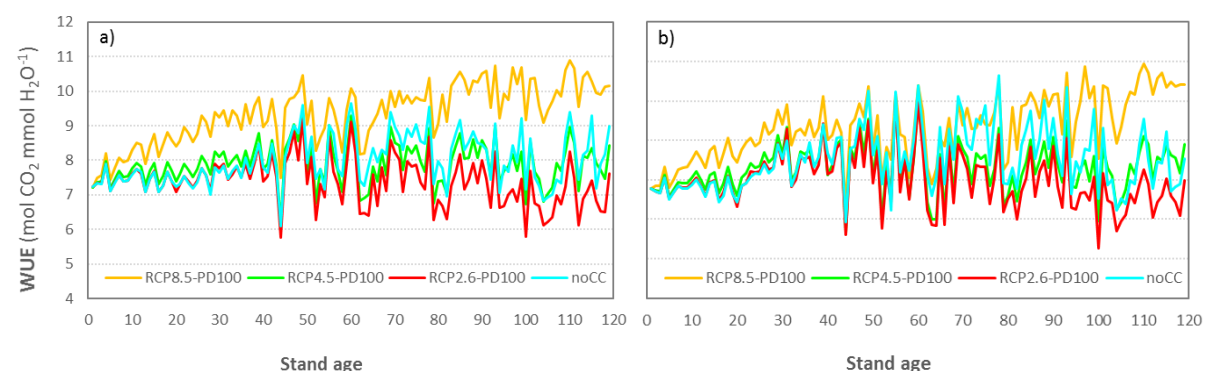


Figure S8. Four climate scenarios (noCC, RCP2.6, RCP4.5, RCP8.5) with increasing CO₂ concentration on water-use efficiency with 100% photosynthetic downregulation of beech (a) and fir (b)). The climate scenario noCC is displayed for comparison assuming no change in precipitation and temperature and

constant CO₂ concentration. The climate data was generated with an in-built weather generator in GOTILWA+ with climate data of the past 40 years from a nearby meteorological weather station. The simulations started with juvenile forests (stand age 0), which corresponds to simulation year 2000.

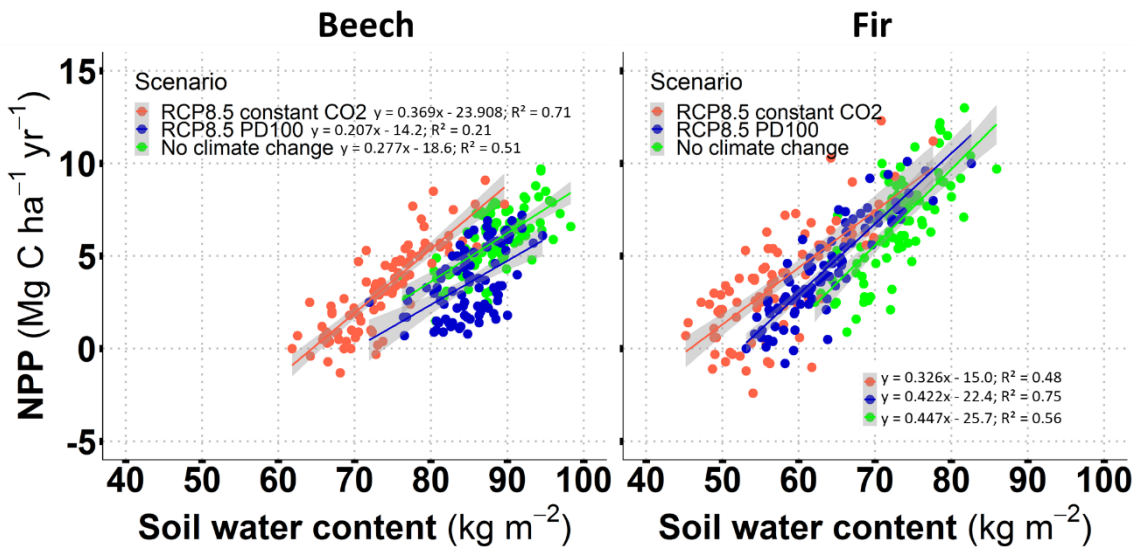


Figure S9. Relationship of net primary productivity (NPP) with soil water content (SWC) for beech and for fir for three scenarios no climate change (reference scenario) and RCP8.5 with constant CO₂ (370ppm) and RCP8.5 with photosynthetic downregulation of 100% (PD100).

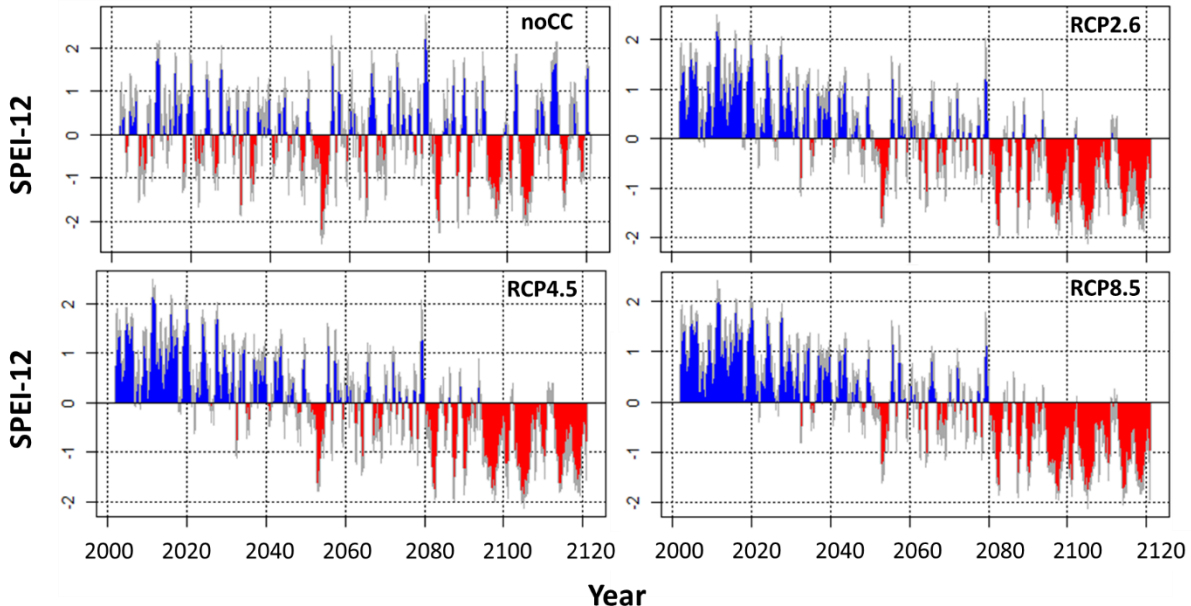


Figure S10. Monthly Standardized Precipitation Evapotranspiration Index (SPEI) of the climate scenarios no climate change (noCC), RCP2.6, RCP4.5 and RCP8.5. Positive values indicate that the difference between monthly precipitation and potential evapotranspiration is larger than the average for a given monthly period. Negative values thus represent conditions drier than average. The monthly periods used were 3, 6, 12 and 24 months for SPEI-3, SPEI-6, SPEI-12 and SPEI-24, respectively.

Supplementary Tables

Table S1. Parameters of beech and fir used for different submodules (**a-g**) in GOTILWA+. Reference indicates the source of the used parameter originating from a pre-setting of GOTILWA+ (GOT), the Freiamt experimental site (FRA), measured parameter (meas), calibrated parameter of a pre-setting of GOTILWA+ (cal), setting by the user (user). For alometric relationships and wood density in (**e**) following references were used [1], [2], [3], [4], [5], [6].

Parameters for different GOTILWA+		Beech	Fir	Unit	Reference
Modules (a-g)					
a) Constants					
PAR to global radiation	0.42	0.42	joule/joule	GOT	
μ Einstens per watt	4.6	4.6	μ E/watt	GOT	
Energy equivalence of organic matter	4700	4700	cal/g	GOT	
Organic matter to carbon ratio	2	2	g/g	GOT	
grams of N per 100 g of dry matter	1.2	1.2	g/g	GOT	
Respiration rate of structural components					
25°C	33.3	33.3	cal/g/d	GOT	
Respiration rate of non-structural components 25°C	55.5	55.5	cal/g/d	GOT	
Respiration rate of living components of wood 25°C	35	35	cal/g/d	GOT	
Plant tissues formed by 1 g of carbon	0.68	0.68	g/g	GOT	
b) Canopy structure					
Longitude	7.93	7.93	GG.mm	FRA	
Latitude	48.2	48.2	GG.mm	FRA	
Altitude	481	481	m a.s.l.	FRA	
Slope	36	9	%	FRA	
Aspect	17.5	17.5	°	FRA	
Albedo of the canopy	0.15	0.076	-	GOT	
Leaf PAR absorbance	0.92	0.92	-	GOT	
Value X for the ellipsoidal distribution	1.35	1.34	-	GOT	
b) Photosynthesis					
V_{cmax} at 25°C	40	40	μ mol/m ² /s	meas	
EaV _{cmax}	75400	75400	J/mol	GOT	
EdV _{cmax}	175000	175000	Ppmv	GOT	
V_{omax} at 25°C	8.4	8.4	μ mol/m ² /s	GOT	
EaV _{omax}	75400	75400	J/mol	GOT	
EdV _{omax}	175000	175000	Ppmv	GOT	
J_{max} at 25°C	70	75	μ mol/m ² /s	meas	
EaJ _{max}	65300	65300	J/mol	GOT	
EdJ _{max}	129000	129000	J/mol	GOT	
SJ _{max}	420	420	J/mol/°K	GOT	
Curvature of the function A_n/PPFD	0.7	0.7	-	meas	
K _c at 25°C	404	404	Pa	GOT	
EaK _c	59400	59400	J/mol	GOT	
K _o at 25°C	248000	248000	Pa	GOT	
EaK _o	36000	36000	J/mol	GOT	

Compensation point (Γ^*) at 25°	42.2	42.2	$\mu\text{mol/mol}$	GOT
EaGammast	37830	37830	J/mol	GOT
R _d at 25°C	0.69	0.57	$\mu\text{mols/m}^2/\text{s}$	meas
Q ₁₀ value at 25°C	2.2	2.2	-	GOT
Mesophyll conductance	Unlimited	Unlimited	-	GOT

c) Stomatal conductance (g_s)

Residual conductance	0.01	0.01	$\text{mols/m}^2/\text{s}$	GOT
Leuning constant (g_1)	7	7	-	GOT
Factor reflecting g_s vs. VPD responses ($g_{s,\text{DO}}$)	0.8	0.8	-	cal
$W_{\text{fac.}}$			-	
Soil water content (SWC) at which $g_s=0$	15	20	m^3/m^3	cal
SWC at which $g_s=g_{s,\text{max}}$	65	65	m^3/m^3	cal
Curvature (q) for photosynthetic response function	0.6	0.4	-	GOT
Leaf characteristical dimension	0.002	0.002	m	GOT
Parameter X for the ellipsoidal distribution	1.35	1.34	v/h	GOT
Diferencial transpiration rate (tall-short trees)	1.025	1.025	-	GOT
Trees leaf stomatal type	Hypostomatou s	Hypostomatou s	-	User

d) Volatile Organic Compounds (VOC)

VOC emissions	Monoterpenes	Isoprene & Monoterpene	User
VOC emission model	Niinemets	Niinemets	User
Isoprens basal emission rate	-	0.00416295	$\mu\text{gramm C/g/h}$
Monoterpen basal emission rate	0.01665182	4.829028	$\mu\text{mols C/g/h}$

e) Tree structure

Alometric relationships

i) DBH - total aboveground biomass	$y = a * \text{DBH}^b$		<i>Beech</i>	<i>Fir</i>
a	0.125	0.1122	-	[1] [2]
b	2.2215	2.36	-	[1] [2]
ii) DBH - bark thickness	$y = a * \text{DBH}^b$			
a	0.04938	0.049	-	GOT
b	0.9196	0.9	-	GOT
			<i>Beech</i>	<i>Fir</i>
Wood density	0.6	0.39	g/cm^3	[3, 4, 5] [5, 6]
Bark density	0.44	0.38	g/cm^3	GOT
Morphic coefficient (tapering)	0.51	0.83	-	cal
Leaf area index in closed mature forests	7.5	10	m^2/m^2	meas & cal
Leaf mass per area	5.72	12	mg/cm^2	meas & cal
Mean leaf life span	1	5	years	
Maximum mobile carbon stored in leaves	0.17	0.2	%	cal
Sapwood area in closed forests	20	22	m^2/ha	cal
Sapflow treshold for cavitation	12	14	$\text{kg/cm}^2/\text{year}$	GOT
Fraction of respiring sapwood	0.06	0.06	%	GOT

Maximum mobile carbon stored in woody organs	0.2	0.2	%	Cal
Biomass of branches / Aboveground Biomass	0.18	0.2	kg/kg	Cal
Fine roots biomass in closed mature forests	280	310	g/m ²	
P/B of fine roots in closed mature forests	1	3	year ⁻¹	GOT
Belowground /Aboveground biomass	0.133	0.153	kg/kg	Cal
Gross litterfall/fine litterfall	9	10	g/kg/year	GOT
Regeneration tree species	Seedler	Seedler	-	

f) Thermal inertia for photosynthesis and SOM decomposition

Min. temperature treshold for photosynthesis	9	10	°C	cal
Max. temperature treshold for photosynthesis	15	15	°C	cal
Thermal inertia for photosynthesis	3	3	-	cal
Min temperature treshold for SOM decomposition	9	10	°C	cal
Max temperature treshold for SOM decomposition	15	15	°C	cal
Thermal inertia for SOM decomposition	3	3	-	cal

g) Soil Carbon efflux and Hydrology

Initial L+F soil organic matter (SOC)	3268	2400	g/m ²	meas
SOC (% dry weight) in the top layer of mineral soil	5.36	5.00	%	
Bulk density (soil column average)	1.96	1.97	g/cm ³	
Maximum soil water holding capacity	119.35	114.62	Mm	
k (L+F)	0.0066	0.0066	day ⁻¹	GOT
k (A+B)	0.00005	0.0005	day ⁻¹	GOT
Soil Q10	2.2	2.2	-	GOT
L+F to A+B transfer rate	1	1	-	GOT
W min	10	10	mm	GOT
W max	100	100	mm	GOT
Mean soil depth	0.8	0.8	m	meas
Relative volume of stones	32.5	33.0	%	meas
Field capacity (% of max. water filled porosity)	70	70	%	GOT
Drainage rate	0.22	0.22	1/day	GOT

h) Tree density

Un- or evenaged population	unevenaged	unevenaged		user
Response factor to canopy opening	2	2	-	GOT
Mobile C threshold for mortality	30	20	%	cal
DBH classes	2	2	cm	user
Initial DBH	0	0	cm	user
Initial tree density	1200	250	trees/ha	user
Trees per DBH class				
0-2	300	250	-	user
2-4	400	0	-	user
4-6	500	0	-	user

Table S2. Table displaying management interventions in GOTILWA+ for beech (**a**) and fir (**b**) with the year of intervention, the DBH class of intervention (small, big or all DBH classes), the mode of thinning (trees, basal area, standing volume, or biomass), the intensity of thinning (positive signs indicated the number of thinned trees and negative signs the tree number of the remaining stand after thinning), number of regenerated trees (regeneration), and the total tree number of the stand. Interventions are every five years except for the initialisation period (first 35 years). During the initialisation period a diameter distribution was created calibrated with inventory data from Freiamt.

a) European Beech

Year	DBH classes	Thinning Mode	Thinning Intensity	Regeneration	Tree Number
2	All	trees	-500	200	875
6	Big	trees	250	220	823
10	All	trees	-700	200	900
14	All	trees	-700	200	901
16	Big	trees	5	100	941
18	Big	trees	5	70	1006
20	All	trees	-700	70	787
25	All	trees	-650	70	720
30	All	trees	-650	70	720
35	All	trees	-620	70	689
40	All	trees	-600		597
45	All	trees	-550		552
50	All	trees	-530		529
55	All	trees	-500		499
60	All	trees	-450		450
65	All	trees	-400		400
70	All	trees	-350		347
75	All	trees	-300		303
80	All	trees	-255		257
85	All	trees	-220		219
90	All	trees	-195		194
95	All	trees	-175		176
100	All	trees	-161		161
105	All	trees	-147	400	547
110	Big	trees	3	400	796
115	Big	trees	3	400	1115
120	Big	trees	3		1112

b) Silver Fir

Year	DBH classes	Thinning Mode	Thinning Intensity	Regeneration	Tree Number
2	trees	Big	50	800	1000
4	trees	Big	50	900	1850
6	trees	Small	600	0	1250
8	trees	Small	300	300	1250
10	trees	Small	250	250	1250
12	trees	All	200	250	1340

14	trees	All	200		1071
16	trees	All	100	100	1071
18	trees	All	100		980
20	trees	All	50	100	1030
25	trees	All	-800	100	900
30	trees	All	-750	50	800
35	trees	All	-700	50	750
40	trees	All	-650		649
45	trees	All	-562		562
50	trees	All	-495		496
55	trees	All	-437		436
60	trees	All	-389		388
65	trees	All	-345		344
70	trees	All	-296		295
75	trees	All	-256		257
80	trees	All	-220		221
85	trees	All	-189		190
90	trees	All	-163		162
95	trees	All	-138		139
100	trees	All	-115	100	214
105	trees	Big	15	50	249
110	trees	Big	15	50	237
115	trees	Big	17	50	270
120	trees	Big	10	50	270

Table S3. Natural data per ha of business-as-usual simulations (noCC) at 5 year cycles for beech (**a**) and fir (**b**) displaying the tree number (N), standing volume (over bark), harvesting volume (over bark), diameter at breast height (DBH), height (H), basal area (BA), current annual increment (CAI), mean annual increment (MAI), total accumulated growth (TAG), total biomass (TBM, above- and belowground), deadwood volume (DWV), and number of dead trees (mortality).

a) European Beech

Stand age yr	N	SV m ³	HV m ³	DBH cm	H m	BA m ²	CAI m ³ yr ⁻¹	MAI m ³ yr ⁻¹	TAG m ³	TBM t	DWV m ³	Mortality
5	793	7	0	6.4	7.1	2.8	0.0	17	10	12	0.009	82
10	900	9	7	7.0	9.1	3.1	2.6	26	17	16		
15	845	27	7	9.1	11.0	5.4	3.4	52	25	33	0.006	56
20	787	41	16	9.2	8.9	6.8	4.2	83	43	49	0.001	11
25	720	71	14	11.7	13.3	9.3	5.2	129	58	67		
30	720	118	10	12.6	13.8	12.9	6.2	186	68	98	0.004	11
35	689	146	23	15.0	15.9	14.8	6.8	238	93	122		
40	597	196	21	16.8	17.2	17.7	7.8	311	116	153	0.002	22
45	552	214	17	18.4	18.6	18.3	7.7	348	135	179		
50	529	296	13	21.1	20.4	23.2	8.9	445	148	219		
55	499	328	18	22.6	21.4	24.5	9.0	496	168	238		
60	450	353	35	24.3	22.6	25.1	9.3	558	205	251		
65	400	354	39	25.5	23.4	24.3	9.2	601	247	248		
70	347	366	53	27.3	24.7	23.7	9.6	670	305	251		
75	303	380	51	29.2	26.1	23.3	9.9	739	359	257		
80	257	380	62	31.0	27.3	22.1	10.1	806	426	251		
85	219	360	61	32.4	28.3	20.2	10.0	851	492	236		
90	194	375	47	34.4	29.8	19.9	10.2	917	543	242		
95	176	389	35	36.1	30.9	19.7	10.2	969	581	246		
100	161	405	36	37.8	32.1	19.7	10.2	1024	619	253		
105	547	374	35	38.8	32.8	19.6	9.8	1030	656	249		
110	796	361	40	39.2	33.6	19.3	9.6	1060	699	250	0.016	148
115	1115	368	51	40.4	34.9	20.0	9.8	1122	754	256	0.008	78
120	1115	405	0	41.9	35.9	21.8	9.7	1159	754	282		

b) Silver Fir

Stand age yr	N	SV m ³	HV m ³	DBH cm	H m	BA m ²	CAI m ³ yr ⁻¹	MAI m ³ yr ⁻¹	TAG m ³	TBM t	DWV m ³	Mortality
5	1850	12	0	2.5	6.3	0.3	0.3	0.8	3.1	3	0	
10	1250	15	0	4.5	9.2	2.7	2.8	3.1	27.8	16	0	
15	1071	21	8	7.7	13.6	5.4	7.5	5.6	78.3	36	0.046	269
20	1030	64	16	9.3	14.7	8.9	12.1	7.9	149.2	73	0	
25	900	126	30	12.9	18.5	12.0	16.7	10.2	245.5	134	0	
30	800	190	33	14.2	18.9	15.6	21.7	12.6	365.9	181	0	
35	750	241	31	16.9	21.3	18.6	23.2	14.0	477.6	223	0	
40	649	309	25	19.5	23.3	22.2	22.4	15.1	589.9	268	0.013	51
45	562	332	45	21.5	24.8	22.9	21.0	15.6	687.3	307	0	
50	496	377	44	24.1	26.5	24.9	22.3	16.6	813.0	346	0	
55	436	390	47	26.0	27.7	25.0	19.1	16.3	878.7	347	0	

60	388	414	43	28.1	29.0	25.7	16.8	16.6	981.1	370	0
65	344	412	47	29.7	29.9	25.1	18.0	16.5	1058.9	379	0
70	295	422	60	32.2	31.3	25.0	17.8	16.8	1159.3	399	0
75	257	432	57	34.6	32.6	25.0	20.7	17.1	1265.8	410	0
80	221	423	61	36.7	33.7	24.0	21.3	17.4	1372.1	424	0
85	190	408	60	38.7	34.8	22.8	16.9	17.1	1435.1	405	0
90	162	404	61	41.5	36.2	22.2	16.7	17.3	1539.1	413	0
95	139	388	56	43.8	37.3	21.1	18.7	17.3	1622.6	405	0
100	214	361	68	46.5	38.4	20.0	16.9	17.3	1708.5	402	0
105	249	314	68	46.7	38.6	17.5	14.2	17.0	1764.9	366	0
110	237	281	71	48.0	39.3	15.8	11.7	16.7	1825.4	329	0.01
115	270	246	78	50.2	40.2	14.0	15.7	16.9	1922.1	310	0
120	270	280		53.3	41.5	16.0	18.1	16.8	1986.1	262	0

Table S4. Time table displaying stem density (N), standing volume (SV in $m^3 ha^{-1}$), harvesting volume (HV in $m^3 ha^{-1}$), total accumulated growth (TAG in $m^3 ha^{-1}$), diameter at breast height (DBH in cm), tree height (H in m) and basal area (BA in m^2) of one rotation length of beech (**a**) and fir (**b**) simulated with GOTILWA+ assuming no climate change (noCC), climate change with RCP 2.6, RCP 4.0 and RCP 8.5 (changes in temperature, precipitation and CO₂ as in Table S1). The thinning intensity for the three climate change scenarios was applied via stem number reductions keeping the same tree density at each interval as for the noCC scenario. Age of the stand was zero at the start of the simulation corresponding to year 2000.

a) Beech

Age	No CC						RCP 2.6					RCP 4.5					RCP 8.5								
	N	SV	HV	TAG	BHD	H	BA	SV	HV	TAG	BHD	H	BA	SV	HV	TAG	BHD	H	BA	SV	HV	TAG	BHD	H	BA
5	1200	7	0	17	6.4	7.1	3	7	0	17	6.4	7.1	3	7	0	17	6.5	7.1	3	7	0	17	6.5	7.2	3
10	900	9	7	26	7.0	9.1	3	9	7	27	7.0	9.1	3	9	8	35	7.2	9.3	3	12	8	31	7.7	9.8	4
15	845	27	7	52	9.1	11.0	5	27	7	55	9.1	11.0	5	32	8	59	9.5	11.5	6	43	11	74	9.3	10.6	7
20	728	41	16	83	9.2	8.9	7	41	16	88	9.2	8.9	7	54	21	104	9.8	11.4	8	75	28	137	12.2	13.7	10
25	720	71	14	129	11.7	13.3	9	71	14	140	11.7	13.3	9	91	18	161	12.7	14.1	11	137	27	229	14.6	15.6	15
30	720	114	10	182	12.6	13.8	13	114	10	200	12.6	13.8	13	152	15	239	13.7	14.7	16	237	20	350	17.8	18.0	21
35	689	156	23	248	15.0	15.9	15	156	23	261	15.0	15.9	15	199	28	317	16.4	16.9	18	290	43	449	18.8	18.6	24
40	597	196	21	311	16.8	17.2	18	196	21	330	16.8	17.2	18	238	28	386	17.5	17.7	20	335	46	544	19.4	18.9	26
45	544	214	17	348	18.4	18.6	18	214	17	384	18.4	18.6	18	272	23	444	19.4	19.1	22	379	34	625	21.4	20.4	27
50	529	296	13	445	21.1	20.4	23	296	13	448	21.1	20.4	23	334	10	518	21.6	20.7	25	455	20	723	23.7	22.0	31
55	499	328	18	496	22.6	21.4	25	328	18	485	22.6	21.4	25	357	20	562	22.8	21.5	26	485	27	781	25.0	23.3	31
60	450	353	35	558	24.3	22.6	25	353	35	534	24.3	22.6	25	375	35	618	24.3	22.5	26	499	48	847	26.4	24.7	31
65	400	354	39	601	25.5	23.4	24	354	39	553	25.5	23.4	24	348	46	641	24.9	23.0	24	466	60	879	27.1	25.4	28
70	347	366	53	670	27.3	24.7	24	366	53	603	27.3	24.7	24	361	43	700	26.6	24.4	23	478	59	955	28.7	27.2	27
75	303	380	51	739	29.2	26.1	23	380	51	655	29.2	26.1	23	353	61	758	28.1	25.7	22	477	69	1028	30.3	29.0	25
80	257	380	62	806	31.0	27.3	22	380	62	694	31.0	27.3	22	338	56	803	29.4	26.8	20	457	73	1086	31.7	30.5	23
85	219	360	61	851	32.4	28.3	20	360	61	727	32.4	28.3	20	330	44	843	30.8	27.9	19	405	69	1108	33.1	31.8	21
90	194	375	47	917	34.4	29.8	20	375	47	783	34.4	29.8	20	347	46	909	32.9	29.5	18	429	55	1191	35.6	34.6	20
95	176	389	35	969	36.1	30.9	20	389	35	823	36.1	30.9	20	363	32	959	34.7	30.8	18	430	36	1232	37.1	35.9	20
100	161	405	36	1024	37.8	32.1	20	405	36	853	37.8	32.1	20	363	32	993	35.8	31.6	18	417	36	1257	38.0	36.7	19
105	147	374	35	1030	38.8	32.8	20	374	35	871	38.8	32.8	20	333	29	995	36.7	32.2	18	403	35	1280	38.8	37.4	19
110	144	361	40	1060	39.2	33.6	19	361	40	902	39.2	33.6	19	323	40	1027	37.0	33.0	18	393	47	1320	39.3	38.7	19

115	141	368	51	1122	40.4	34.9	20	368	51	932	40.4	34.9	20	306	42	1056	37.1	33.7	17	364	49	1344	39.2	39.3	19
120	141	405	0	1159	41.9	35.9	22	405	0	955	41.9	35.9	22	327	0	1076	38.0	34.3	19	376	0	1356	39.7	39.7	20

a) Fir

Age	No CC							RCP 2.6					RCP 4.5					RCP 8.5							
	N	SV	HV	TAG	BHD	H	BA	SV	HV	TAG	BHD	H	BA	SV	HV	TAG	BHD	H	BA	SV	HV	TAG	BHD	H	BA
5	1850	12	0	16	2.5	6.3	0	12	0	12	3.5	8.4	0	12	0	12	3.5	8.4	0	12	0	12	3.6	8.6	0
10	1250	15	0	19	4.5	9.2	3	19	0	23	5.5	11.0	3	19	0	23	5.6	11.1	3	19	0	23	6.0	11.5	3
15	1071	21	8	30	7.7	13.6	5	26	9	41	7.9	13.8	6	31	11	47	8.8	15.0	6	48	17	72	8.6	14.5	7
20	1030	64	16	91	9.3	14.7	9	71	17	105	10.6	16.5	9	81	19	120	10.8	16.7	10	119	28	175	11.0	16.1	13
25	900	126	30	188	12.9	18.5	12	144	32	216	13.3	18.8	13	145	43	233	13.7	19.1	13	207	62	330	15.5	20.5	17
30	800	190	33	289	14.2	18.9	16	216	22	314	16.3	21.3	18	232	30	355	16.6	21.3	18	310	53	494	17.0	20.8	23
35	750	241	31	376	16.9	21.3	19	273	33	409	17.9	22.2	20	294	37	458	18.3	22.4	21	394	49	635	20.2	23.5	27
40	649	309	25	472	19.5	23.3	22	324	23	486	20.1	24.0	23	353	23	543	20.8	24.2	25	430	57	736	21.5	24.2	29
45	562	332	45	547	21.5	24.8	23	334	45	548	21.8	25.2	23	365	50	614	22.6	25.5	25	452	62	829	23.8	25.8	29
50	496	377	44	642	24.1	26.5	25	361	43	623	23.9	26.6	24	396	45	696	24.8	26.9	26	492	59	936	26.4	27.5	31
55	436	390	47	709	26.0	27.7	25	367	41	677	25.5	27.6	24	404	49	759	26.5	28.0	26	501	60	1015	28.3	28.7	0
60	388	414	43	782	28.1	29.0	26	379	43	737	27.3	28.7	24	422	42	825	28.5	29.2	26	526	58	1105	30.7	30.1	31
65	344	412	47	833	29.7	29.9	25	361	39	765	28.2	29.2	23	401	45	856	29.4	29.7	25	504	55	1145	31.8	30.8	29
70	295	422	60	912	32.2	31.3	25	359	51	821	30.1	30.3	22	394	59	916	31.4	30.8	24	494	73	1219	33.9	32.2	28
75	257	432	57	988	34.6	32.6	25	351	50	870	31.9	31.3	21	391	53	973	33.3	31.9	23	480	65	1280	35.9	33.5	27
80	221	423	61	1048	36.7	33.7	24	335	47	908	33.3	32.1	20	370	54	1014	34.8	32.7	21	458	63	1330	37.6	34.5	25
85	190	408	60	1101	38.7	34.8	23	323	44	946	35.0	33.0	19	351	50	1053	36.5	33.6	20	433	65	1378	39.3	35.6	23
90	162	404	61	1168	41.5	36.2	22	320	49	1000	37.5	34.4	18	363	50	1121	39.6	35.2	20	445	66	1465	42.9	37.7	23
95	139	388	56	1215	43.8	37.3	21	305	45	1036	39.3	35.3	17	343	53	1162	41.7	36.2	19	411	61	1502	44.7	38.6	21
100	114	361	68	1267	46.5	38.4	20	278	50	1066	41.1	36.1	15	309	57	1193	43.4	37.0	17	365	63	1527	46.1	39.4	19
105	99	314	68	1297	46.7	38.6	17	244	50	1089	41.4	36.2	14	271	56	1219	43.9	37.1	15	317	71	1560	46.2	39.5	17
110	84	281	71	1345	48.0	39.3	16	219	51	1122	42.5	37.0	12	249	59	1263	45.5	38.0	14	293	75	1622	48.1	40.7	16
115	67	246	78	1399	50.2	40.2	14	183	54	1147	43.6	37.6	11	216	63	1303	47.4	38.7	12	246	78	1663	49.3	41.2	14
120	67	280	0	1434	53	42	16	217	0	1181	47.3	39.1	13	249	220	1336	50.8	40.1	15	288	258	1704	53.0	43.0	16

Supplementary Notes

Note S1: Leaf Sampling and Leaf Morphology

We sampled twigs with a tree climber from the top crown in two measurement campaigns (08.06.–16.06.2017 and 10.08.–18.08.2017). The twigs were immediately re-cut under water in the field and stored in water buckets during gas exchange experiments (approximately two hours after cutting). Previous-year twigs of *A. alba* were used for the measurements. Twigs were positioned in the middle of the leaf cuvette avoiding gaps and overlays of needles sealing the gaskets with Blu-tack (Bostik SA, La Plaine St Denis, France). To correct the leaf area, the needles used in gas exchange experiments were collected and scanned to determine their leaf area (LA, cm⁻²) with Adobe Photoshop in the laboratory on the same day (following [7]). 60 leaves for *F. sylvatica* and 120 needles for *A. alba* were collected in sealed plastic bags and measured fresh weight (FW, mg) and LA. After oven-drying the leaves at 60°C for three days we determined dry weight (DW, mg), leaf water content [LWC (%)] = DW*100/FW], the leaf mass per area [LMA (mg cm⁻²) = DW/LA].

Note S2: Photosynthetic Gas Exchange Measurements - CO₂-Response Curves

Foliar gas exchange measurements were carried out with two portable “GFS-3000 gas exchange systems” in parallel with chlorophyll fluorescence measurements on five replicates for each tree species per measurement campaign. We followed the same measurement protocol as in Sperlich et al. (2015b). Only one GFS-3000 was equipped with a “PAM-Fluorometer 3055-FL” (Heinz Walz GmbH, Effeltrich, Germany) reducing *n* for parameters based on chlorophyll fluorescence measurements. Before starting the CO₂-response curves the leaf was kept in darkness for approximately 20 minutes and night respiration (*R_n*) was recorded. The photosynthetic photon flux density (PPFD) was then set to 1000 μmol photons m⁻² s⁻¹. We light-adapted the leaves for 10 minutes and after *A_{net}* and *g_s* values stabilised we started the CO₂-response curves by altering the CO₂ concentrations in the leaf cuvette (*C_a*) stepwise 400 → 300 → 200 → 100 → 50 → 400 → 400 → 600 → 800 → 1000 → 1500 → 2000 μmol CO₂ m⁻² s⁻¹. Acclimation time was 120 seconds between each step [9]. Additionally to the CO₂-response curves we conducted light-response experiments (A/PPFD-curve) for the estimation of mitochondrial respiration of a leaf in light conditions (*R_d*) on several samples of each species using the CF-method as proposed by Yin et al. (2009). See *supplementary material* for details. Prior to our experiments, we tested the cutting-twigs method on *A. alba* and *F. sylvatica*. We found that foliar *A_{net}* and *g_s* of attached intact twigs did not differ significantly (*P*<0.05) to leaves on cut twigs for the period of our response curves (~2 hours) (see *suppl. Material Fig. xx*).

With the chlorophyll fluorescence-derived effective quantum yield of photosystem II (Φ_{PSII}), we estimated *g_m* using the variable-*J* method by Harley et al. (1992):

$$g_m = \frac{A_{net}}{C_i - \frac{[\Gamma^* * J_{CF} + 8(A_{net} + R_d)]}{J_{CF} - 4(A_{net} + R_d)}} \quad (S1)$$

where Γ^* is the CO₂ concentration at which the photorespiratory efflux of CO₂ equals the rate of photosynthetic CO₂ uptake, *R_d* is the mitochondrial respiration of a leaf in light conditions, *J_{CF}*, is the electron-transport rate based on Φ_{PSII} (see *suppl. Material* for details). The chloroplastic CO₂ concentration, *C_c*, was thereafter determined as [*C_c*=*C_i*–*A_{net}*/*g_m*].

Photosynthesis Model

We then fitted the Farquhar, von Caemmerer, and Berry (FvCB) photosynthesis model to the CO₂-response curves based on *C_i* (A/*C_i*-curve) and on *C_c* (A/*C_c*-curve) to determine the ‘apparent’ and

'true' (respectively) maximum rate of Rubisco carboxylation ($V_{c,\max}$), electron-transport rate (J_{\max}) and triose-phosphate use (TPU) [12,13] as in [8,14]. $V_{c,\max}$, J_{\max} and TPU define the biochemical potential of photosynthesis.

Statistical Analyses

The different ecophysiological parameters (A_{net} , g_s , g_m , R_n , R_d , $V_{c,\max}$, J_{\max} , TPU, LMA) were tested with ANOVAs and Tukey's HSD tests for significant differences between the experimental groups seasonal campaigns, species and, for *A. alba*, also leaf position with a significance level of $P \leq 0.05$. Linear regressions were conducted for several parameter combinations, such as A_{net}/g_s , $J_{\max}/V_{c,\max}$, g_s/g_m , and A_{net}/g_m . To compare the difference of the regression slopes, ANCOVAs were used. All statistical analyses were conducted with the R software (Version 3.4.0, R Core Team 2017).

Note S3: LAI Measurements

We used the "LAI-2200C Plant Canopy Analyzer" (Li-Cor Inc., Lincoln, NE, USA) to measure the seasonal course of leaf area index (LAI) in groups of pure beech, pure fir and mixed beech-fir stands at our study site Freiamt. Additionally, we measured the LAI in a total of 40 stands of different age classes in a nearby forest district (Wittnau) ($n=22$ for *F. sylvatica* and $n=18$ for *A. alba*). We chose Wittnau forest district because it is characterised by similar site indices and altitude as our experimental site and it provides many pure stands of *A. alba* and *F. sylvatica* in a wide range of age classes. Also, stand information (location, productivity, yield tables etc.) was available due to a collaboration in an earlier project.

Optical techniques such as the hemispherical images of the LAI-2200C overestimate LAI because signals from woody plant material (branches, twigs, stem etc) are also recorded. We corrected the effective LAI (L_e) for *F. sylvatica* by subtracting the L_e recorded in the leaf-less period in winter in pure *F. sylvatica* stands. In conifer stands, LAI-2200C additionally underestimates LAI because the instrument is sensing projected area of shoots, rather than needles [15,16]. The L_e is thus corrected for the woody-to-total leaf area ratio and the clumping of needles into shoots and branches as in [17]

$$\text{LAI} = \frac{(1 - \beta) \cdot L_e \cdot \gamma_E}{\Omega_E} \quad (\text{S2})$$

where β is the woody-to-total leaf area ratio, L_e is the effective LAI as measured by the LAI-2200C, γ_E is the needle-to-shoot area ratio and Ω_E is the element clumping index. We used β , Ω_E and γ_E from *Picea abies* because no data for *A. alba* was available and multiplied L_e with the correction factor 1.65 [18,19]. We masked the outer 2 rings and used only the three upper rings ($0 \pm 43^\circ$ from zenith) of the hemispherical sensor for LAI as in [20]. The outer one or two rings can be sensitive to the impact of scattered light, even under diffuse sky conditions, or to gap fraction saturation and are frequently excluded from analysis of LAI-2000 data [21–23].

Note S4: GOTILWA+: Productivity, Drought and Mortality

The photosynthesis model from Farquhar-vonCaemerer-Bell (FvCB) [12] calculates the foliar net assimilation rates depending on intercepted quantum flux density, leaf temperature, intercellular CO₂ concentration (C_i) and photosynthetic potentials and is coupled to the Leuning et al. stomatal conductance model [24] to calculate gas exchange rates and C_i. The species-specific photosynthetic potential is critical for the assimilatory efficiency of leaf tissue and is defined by three major processes: maximum carboxylation rate of Rubisco ($V_{c,\max}$), maximum rate of electron transport (J_{\max}) and triose-phosphate use (TPU). A two-layer canopy microclimate model scales photosynthesis for sunlit and shaded leaves - with the amount of intercepted diffuse and direct radiation depending on the time of the day, season, and the area of leaf exposed to the sun [25] – to the whole canopy to calculate bulk gross primary production (GPP). NPP is calculated from GPP minus maintenance respiration (MR). GOTILWA+ assumes a rate of 0.32 gC lost by growth respiration (GR;[26]) per 1 gC of NPP invested

in growth. The assimilated carbon is allocated to leaf, sapwood and fine roots – each with a temperature-dependant respiration rate. Leaf biomass depends on the ratio of leaf mass per leaf area (LMA, g cm⁻²) and the maximum leaf area of a stand expressed as leaf area per ground area (leaf area index, LAI in m² m⁻²).

Simulation of Drought in GOTILWA+

Water stress directly reduces the photosynthetic potential through a nonlinear relation to soil water content by using an empirical β coefficient [27,28]. When the leaf respiration rate exceeds the photosynthetic assimilation rate and the mobile carbon pools are exhausted, a number of leaves are shed until the carbon balance is positive. In spring, evergreen trees then produce new leaves when photosynthesis has recharged mobile carbon pools being expended in winter to maintain the living biomass. Deciduous trees unfold leaves in 10 days when the stage of development imposes values of photosynthesis higher than 90% of optimal condition. Leaf fall occurs gradually when day length is decreasing and the stage of development imposes values of photosynthesis lower than 95% of optimal condition.

Mortality Submodule

When NPP in GOTILWA+ turns negative due to insufficient carbon assimilation (e.g. stomatal closure under drought), the mobile carbon pool is gradually depleted for maintenance and/or growth respiration inducing eventually leaf shedding and die-off of fine roots to restore the balance in the carbon budget. Tree mortality occurs when the trees in a diameter class are completely defoliated and the mobile carbon pool falls below a specific threshold (Table S1h - mobile C threshold for mortality) – which is a percentage of the plant's total mobile carbon pool set by the user. Tree number is reduced until the balance of demand and supply of carbohydrates is restored. See [29] and [30] for further details on the mortality sub-model of GOTILWA+.

Reference

1. Zell, J.; Bösch, B.; Kändler, G. Estimating above-ground biomass of trees: comparing Bayesian calibration with regression technique. *Eur. J. For. Res.* **2014**, *133*, 649–660, doi:10.1007/s10342-014-0793-7.
2. Nord-Larsen, T.; Nielsen, A.T. Biomass, stem basic density and expansion factor functions for five exotic conifers grown in Denmark. *Scand. J. For. Res.* **2015**, *30*, 135–153, doi:10.1080/02827581.2014.986519.
3. Gebauer, T.; Horna, V.; Leuschner, C. Variability in radial sap flux density patterns and sapwood area among seven co-occurring temperate broad-leaved tree species. *Tree Physiol.* **2008**, *28*, 1821–30, doi:10.1093/TREEPHYS/28.12.1821.
4. Vejpustková, M.; Zahradník, D.; Čihák, T.; Šrámek, V. Models for predicting aboveground biomass of European beech (*Fagus sylvatica* L.) in the Czech Republic. *J. For. Sci.* **2015**, *61*, 45–54, doi:10.17221/100/2014-JFS.
5. Brzeziecki, B.; Kienast, F. Classifying the life-history strategies of trees on the basis of the Grimian model. *For. Ecol. Manage.* **1994**, *69*, 167–187, doi:10.1016/0378-1127(94)90227-5.
6. EOL European Silver Fir - Encyclopedia of Life Available online: <https://eol.org/pages/1033070> (accessed on 23 March 2020).
7. Sperlich, D.; Chang, C.T.; Peñuelas, J.; Gracia, C.; Sabaté, S. Seasonal variability of foliar photosynthetic and morphological traits and drought impacts in a Mediterranean mixed forest. *Tree Physiol.* **2015**, *35*, 501–520, doi:10.1093/treephys/tpv017.
8. Sperlich, D.; Chang, C.T.; Peñuelas, J.; Gracia, C.; Sabaté, S. Seasonal variability of foliar photosynthetic and morphological traits and drought impacts in a Mediterranean mixed forest. *Tree Physiol.* **2015**, *35*, 501–520,

- doi:10.1093/treephys/tpv017.
- 9. Long, S.P.; Bernacchi, C.J. Gas exchange measurements, what can they tell us about the underlying limitations to photosynthesis? Procedures and sources of error. *J. Exp. Bot.* **2003**, *54*, 2393–401, doi:10.1093/jxb/erg262.
 - 10. Yin, X.; Struik, P.C.; Romero, P.; Harbinson, J.; Evers, J.B.; Van Der Putten, P.E.L.; Vos, J. Using combined measurements of gas exchange and chlorophyll fluorescence to estimate parameters of a biochemical C photosynthesis model: a critical appraisal and a new integrated approach applied to leaves in a wheat (*Triticum aestivum*) canopy. *Plant, Cell Environ.* **2009**, *32*, 448–64, doi:10.1111/j.1365-3040.2009.01934.x.
 - 11. Harley, P.C.; Loreto, F.; Di Marco, G.; Sharkey, T.D. Theoretical Considerations when Estimating the Mesophyll Conductance to CO₂ Flux by Analysis of the Response of Photosynthesis to CO₂. *Plant Physiol.* **1992**, *98*, 1429–1436.
 - 12. Farquhar, G.D.; von Caemmerer, S.; Berry, J.A. A Biochemical Model of Photosynthesis CO₂ Assimilation in Leaves of C3 Species. *Planta* **1980**, *149*, 78–90.
 - 13. Sharkey, T.D. Photosynthesis in intact leaves of C3 plants: Physics, physiology and rate limitations. *Bot. Rev.* **1985**, *51*, 53–105.
 - 14. Sperlich, D.; Barbata, A.; Ogaya, R.; Sabate, S.; Penuelas, J. Balance between carbon gain and loss under long-term drought: impacts on foliar respiration and photosynthesis in *Quercus ilex* L. *J. Exp. Bot.* **2016**, *67*, 821–833, doi:10.1093/jxb/erv492.
 - 15. Gower, S.T.; Norman, J. Rapid estimation of leaf area index of conifer and broad-leaf plantation. *Ecology* **1991**, *72*, 1896–1990.
 - 16. Smolander, H.; Stenberg, P. Response of LAI-2000 estimates to changes in plant surface area index in a Scots pine stand. *Tree Physiol.* **1996**, *16*, 345–349, doi:10.1093/treephys/16.3.345.
 - 17. Chen, J.; Govind, a; Sonnentag, O.; Zhang, Y.; Barr, a; Amiro, B. Leaf area index measurements at Fluxnet-Canada forest sites. *Agric. For. Meteorol.* **2006**, *140*, 257–268, doi:10.1016/j.agrformet.2006.08.005.
 - 18. Pokorný, R.; Tomášková, I.; Havránková, K. Temporal variation and efficiency of leaf area index in young mountain Norway spruce stand. *Eur. J. For. Res.* **2008**, *127*, 359–367, doi:10.1007/s10342-008-0212-z.
 - 19. Pokorný, R.; Marek, M.V. Test of Accuracy of LAI Estimation by LAI-2000 under Artificially Changed Leaf to Wood Area Proportions. *Biol. Plant.* **2000**, *43*, 537–544, doi:10.1023/A:1002862611176.
 - 20. Dufrêne, E.; Bréda, N. Estimation of deciduous forest leaf area index using direct and indirect methods. *Oecologia* **1995**, *104*, 156–162, doi:10.1007/BF00328580.
 - 21. Pearse, G.D.; Watt, M.S.; Morgenroth, J. Comparison of optical LAI measurements under diffuse and clear skies after correcting for scattered radiation. *Agric. For. Meteorol.* **2016**, *221*, 61–70, doi:10.1016/j.agrformet.2016.02.001.
 - 22. Chen, J.M.; Leblanc, S.G. Multiple-scattering scheme useful for geometric optical modeling. *IEEE Trans. Geosci. Remote Sens.* **2001**, *39*, 1061–1071, doi:10.1109/36.921424.
 - 23. Breda, N.J.J. Ground-based measurements of leaf area index: a review of methods, instruments and current controversies. *J. Exp. Bot.* **2003**, *54*, 2403–2417, doi:10.1093/jxb/erg263.
 - 24. Leuning, R. A critical appraisal of a combined stomatal-photosynthesis model for C3 plants. *Plant, Cell Environ.* **1995**, *18*, 339–355, doi:10.1111/j.1365-3040.1995.tb00370.x.
 - 25. Campbell, G.S. Extinction coefficients for radiation in plant canopies calculated using an ellipsoidal inclination angle distribution. *Agric. For. Meteorol.* **1986**, *36*, 317–321, doi:10.1016/0168-1923(86)90010-9.
 - 26. Ovington, J.D. Some Aspects of Energy Flow in Plantations of *Pinus sylvestris* L. *Ann. Bot.* **1961**, *25*, 12–20, doi:10.1093/oxfordjournals.aob.a083728.

27. Keenan, T.; García, R.; Friend, a. D.; Zaehle, S.; Gracia, C.; Sabate, S. Improved understanding of drought controls on seasonal variation in Mediterranean forest canopy CO₂ and water fluxes through combined in situ measurements and ecosystem modelling. *Biogeosciences* **2009**, *6*, 2285–2329, doi:10.5194/bg-6-2285-2009.
28. Drake, J.E.; Power, S.A.; Duursma, R.A.; Medlyn, B.E.; Aspinwall, M.J.; Choat, B.; Creek, D.; Eamus, D.; Maier, C.; Pfautsch, S.; et al. Stomatal and non-stomatal limitations of photosynthesis for four tree species under drought: A comparison of model formulations. *Agric. For. Meteorol.* **2017**, *247*, 454–466, doi:10.1016/j.agrformet.2017.08.026.
29. Nadal-Sala, D.; Keenan, T.F.; Sabaté, S.; Gracia, C. Forest eco-physiological models: water use and carbon sequestration. In *Managing Forest Ecosystems: The Challenge of Climate Change*; Bravo, F., LeMay, V., Jandl, R., Eds.; Springer, 2017; pp. 81–102 ISBN 9783319282503.
30. Bugmann, H.; Seidl, R.; Hartig, F.; Bohn, F.; Brúna, J.; Cailleret, M.; François, L.; Heinke, J.; Henrot, A.-J.; Hickler, T.; et al. Tree mortality submodels drive simulated long-term forest dynamics: assessing 15 models from the stand to global scale. *Ecosphere* **2019**, *10*, e02616, doi:10.1002/ecs2.2616.